Original scientific paper
https://doi.org/10.33180/InfMIDEM2024.201

Informacije MIDEM
Journal of Microelectronics, Electronic Components and Materials
Vol. 54, No. 2(2024), XX – XX

Multi-Beam Metasurface Control Based on Frequency Reconfigurable Antenna

Marwa M. Ismail [1], Bashar Bahaa Qas Elias [2], Taha A. Elwi[3], Bashar S. Bashar [4], Ali Ihsan Alanssari [5], Z.A. Rhazali[6], Halina Misran [7]
[1,2] Department of Information and Communication Engineering, College of Information Engineering, Al-Nahrain University, Jadriya, Baghdad, Iraq
[4,6] Electrical & Electronic Engineering Department College of Engineering Universiti Tenaga Nasional Kajang, Malaysia
[2]International Applied and Theoretical Research Center (IATRC), Baghdad Quarter, Iraq;
[5] Department of Systems Engineering, College of Information Engineering, Al-Nahrain University, Jadriya, Baghdad, Iraq
[7] Nanoarchitectonic Laboratory Department of Mechanical Engineering Universiti Tenaga Nasional Kajang, Malaysia

Abstract: This paper presents a new design and analysis of a reconfigurable antenna with a switchable slot held using PIN diodes for multifunction reconfiguration, including frequency multiplexing. The performance of the proposed antenna in terms of reflection coefficient spectra and radiation patterns is evaluated. From the results obtained, it is observed that the antenna can be operated for different frequencies: 1.8 GHz, 2.7 GHz, 3.1 GHz, 3.3 GHz, 4.1 GHz, 5.1 GHz, and 5.4 GHz. A maximum gain of 11.1 dBi is also significantly achieved at 5.1 GHz. Moreover, this antenna is designed to provide a high Q-factor and low-frequency ratio (FR) for using the spectrum efficiently. Upon the advantage of spatial diversity, multiple independent data streams can be transmitted over the same frequency simultaneously. All results obtained in this work were produced based on the simulation process using CST Microwave Studio simulator software at different switching scenarios.

Keywords: Reflection coefficient, gain, microstrip patch, modes, Metasurface

Več žarčni metapovršinski nadzor na podlagi frekvenčno nastavljive antene

Izvleček: Prispevek predstavlja novo zasnovo in analizo nastavljive antene s preklopno režo z uporabo diod PIN za več funkcijsko nastavljivost, vključno s frekvenčnim multipleksiranjem. Ovrednotena je zmogljivost predlagane antene v smislu spektrov koeficienta odboja in sevalnih vzorcev. Iz dobljenih rezultatov je razvidno, da lahko antena deluje na različnih frekvencah: 1,8 GHz, 2,7 GHz, 3,1 GHz, 3,3 GHz, 4,1 GHz, 5,1 GHz in 5,4 GHz. Pri frekvenci 5,1 GHz je doseženo tudi največje ojačenje 11,1 dBi. Poleg tega je ta antena zasnovana tako, da zagotavlja visok faktor Q in nizko frekvenčno razmerje (FR) za učinkovito uporabo spektra. S prednostjo prostorske raznolikosti je mogoče hkrati prenašati več neodvisnih podatkovnih tokov na isti prosti frekvenci. Vsi rezultati, pridobljeni v tem delu, so bili pridobljeni na podlagi postopka simulacije z uporabo programske opreme CST Microwave Studio pri različnih scenarijih preklapljanja.

Ključne besede: Odbojni koeficient, ojačanje, mikrotrakasta krpica, meta površina

** Corresponding Author's e-mail: bashar.bahaa@nahrainuniv.edu.iq, PE21173@student.uniten.edu.my*

1 Introduction

After years of building high-efficiency transceivers to compensate for signal loss at the ends of a radio channel, designers are now beginning to realize that they have reached the practical limits of transceiver efficiency as they prepare to introduce the 5th generation (5G) technology [1-3]. 5G communication systems must meet a wide range of needs, such as extremely high data rates, high mobility, and low latency unavailable in preexisting networks [4]. 5G technology has some outstanding qualities, which are boosting its adoption. One

Accepted article

of the most notable advantages of 5G is its high data speeds, which surpass 20 Gbps - substantially faster than 4G LTE's 1 Gbps peak. Furthermore, 5G has tremendous mobility, allowing users to maintain lightning-fast speeds even when on the move. Moreover, another major feature of 5G is its incredibly low latency, which is expected to be as low as 1 millisecond, significantly lower than the 50-millisecond delay of 4G. This near-instant reaction time allows for real-time applications such as self-driving cars, which require quick communication. The combination of high data speeds and low latency makes 5G a major change in modern connection. Overall, 5G has greater performance in areas like data rates. Tele-education, virtual reality offices, social media, telemedicine, e-governance, e-commerce, and many other emerging high-data-rate applications will necessitate these standards [5]. A high-gain antenna array is highly desired for such a wide range of applications[6]. Multiple-input multiple-output (MIMO) antennas are utilized to meet the vast need for high-volume data transmission across the communication channel because of their exceptional characteristics, including immunity to multipath fading, low consumption of power compared to data rate, and fast data utilization [7, 8].

Resource allocation in 5G networks can be a complex optimization problem requiring efficient algorithms [9]. One of the most popular approaches is distributed optimization, which involves multiple nodes in the network collaborating to solve the optimization problem [10]. One such algorithm is the Alternating Direction Method of Multipliers (ADMM) [11]. ADMM is a distributed optimization algorithm well-suited for resource allocation problems in communication networks. It is advantageous when the optimization problem can be decomposed into smaller sub-problems [12].

In the context of resource allocation in 5G networks, ADMM can allocate radio resources such as bandwidth and power to different users in the network [13]. The problem can be formulated as a constrained optimization problem, where the objective is to maximize the network throughput subject to constraints on the available resources [14]. The ADMM algorithm involves the following steps: Decompose the problem into smaller sub-problems, each of which can be solved by individual nodes in the network [15]. Each node solves its sub-problem independently and then communicates the solution to its neighbors [2]. The neighboring nodes exchange information and update their solutions accordingly [16, 17]. The process is repeated until convergence [18].

Contemporary portable wireless communication devices need multi-functional antennas adaptable to changing system requirements. The Reconfigurable antennas have received substantial consideration in recent years due to their capability to change electromagnetic wave frequency, polarization, or radiation pattern[19, 20]. In an advanced wireless communication system, multiple antennas are deployed for various application-specific tasks[21]. As a result, the system becomes complex and bulkier. The advanced portable device requires a single radiating structure to operate at multiple frequencies. This led to the development of multiband antennas. These antennas offer only fixed performance and cannot be tuned to the user's request. In such scenarios, the concept of frequency reconfiguration provides an excellent solution. This allows the radiating structure to switch at a frequency based on the antennas, which are significant in 5G and cognitive radio communications technologies[22].

Reconfigurable antennas can be reconfigured regarding operating frequency, polarization, or radiation pattern [7]. Due to the 5G technology demand in beam steering and beam shaping, radiation pattern reconfigurable antennas are vital and are being researched extensively. In 5G technology, the mid-band frequencies are defined from 1 to 6 GHz ,being widely used in many wireless technologies, particularly the Internet of Things applications[23]. Using the mid-band frequencies, low power consumption can be maintained when communicating within a short range of network devices [24]. However, the effectiveness of such systems depends on the level of multipath and interference [25]. Thus, reconfiguration of the radiation patterns of antennas will enable the enhancement of signal strength and transmission efficiency [6]. Pattern reconfiguration antennas are one of the critical technologies for modern telecommunication applications. Pattern reconfigurability is essential with the ability to change the current source distribution on the antenna structure by performing the radiated energy as the beam to the dedicated or specific directions that eventually helps improve the communication's data throughput [26, 27]. The reconfigurable pattern antenna could avoid noise sources by directing null toward interference and radiating the main beam to the desired direction for better coverage improvement. This antenna has advantages with its compact size, small power consumption, and increasing functionality to resolve the burden on today's transmission systems within a confined space[28]. This paper presents a simple, compact, low-cost, parasitic, composite right/left-handed (CRLH) resonator-based reconfigurable antenna exhibiting frequency and pattern diversity. The proposed antenna is suitable for steering omnidirectional radiation patterns into bi-directional and unidirectional end-fire radiation patterns for multiple frequencies.

Accepted article

2 Antenna Configuration

In this work, a reconfigurable antenna is structured based on a truncated patch with slots to realize a primary patch antenna to couple the electromagnetic energy inductively to a second patch antenna based on a fractal geometry of a novel structure. As seen in Figure 1, four PIN diodes are proposed to the primary antenna patch to adapt and adjust (reconfigure) an individual radiator's fundamental operating features to their environment by altering their operating frequencies, impedance, radiation pattern, and polarization separately. The second patch of the antenna is introduced to increase the antenna bandwidth through the effects of the inductive coupling. However, raising the proposed Meta surface (MTS) increases the antenna gain at the desired frequencies.

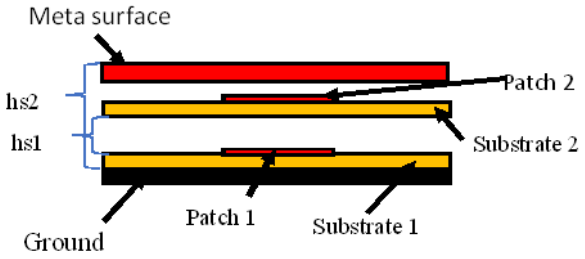

Figure 1: layout of the antenna structure.

The first antenna layer is a microstrip patch with four slots, as seen in Figure 2. These slots are proposed to reduce the effects of surface wave fringing and mitigate the phase retardations from the patch edges. The second layer is designed as a ring of interdigitated capacitors connected to eight fractal patches by T-shaped stubs. The fractal patch also has the advantage of controlling the input impedance matching at the desired resonant frequency through capacitive coupling by directing current to each unit cell. In addition, the proposed MTS is invoked to direct antenna radiation in a specific direction with minimal reflections by gently transferring electromagnetic energy into its free space. This combination realizes the advantages of increasing the antenna bandwidth and gain. In this way, antenna gain is maximized while maintaining the original radiation pattern characteristics of the base station antenna but increasing radiation efficiency and gain. The antenna is printed on a Taconic RF-30 (lossy) substrate with 280×280 mm² of εr=4.4 and 1.6 mm thickness. The entire antenna system height is fixed to 70 mm for maximum gain. The rest of the proposed antenna dimensions are listed in Table 1.

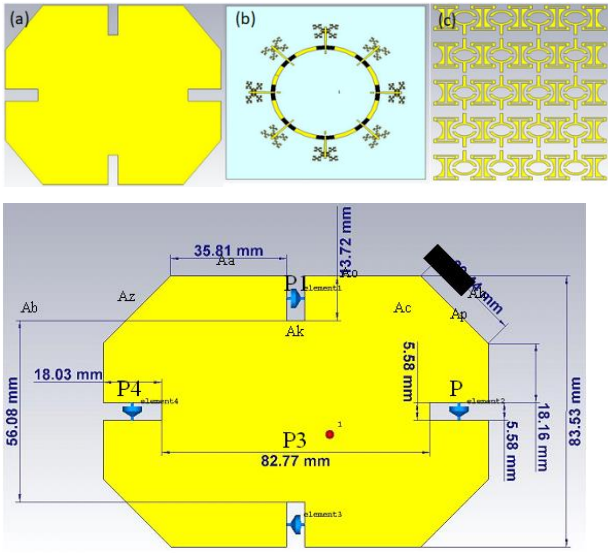

Figure 2: The proposed antenna structure with geometrical details.

Table 1: Overall dimensions of the proposed antenna.

Parameter	Value (mm)	Parameter	Value (mm)
Aa	35.81	Ac	5.58
Az	18.03	As	29.44
Ab	55.08	Ax	83.53
Ao	13.72	Ak	82.77

3 Description of Antenna Layers

The antenna design process and critical parameters leading to the results are elucidated in this section. The outcomes were assessed utilizing CST software employing the Finite Integration Technique (FIT) tailored for microwave devices. A time-domain solver was used in the analysis for wideband or multiband antennas. All dimensions are expressed in millimeters, with the frequency range extending from 0 GHz to 6 GHz, and a parasitic layer is utilized in the suggested design. The study shows that the proposed design enhances gain bandwidth by mitigating conduction and ground plane capacitance losses and suppressing surface waves by incorporating electromagnetic band gap (EBG) defects. The simulation and analysis processes are segmented into the following parts.

3.1 Patch antenna (first layer)

This section presented a parametric study to realize the effects of the proposed shape of the patch on the antenna performance. At this step of design illustrated in Figure 3(a), multiple bands of a traditional rectangular patch are obtained, 9 bands from 3 GHz to 5.7 GHz. Meanwhile, a maximum gain of 11.5 dBi at 4.8 GHz is

Accepted article

observed. Then, it is medicated by cutting the edge of the rectangle, as depicted in Figure 3 (b). Next, in Figure 3(c), the patch structure includes cutting 4 slots from the corners of the radiators with different dimensions. Figure 4(a and b) displays the results of the reflection coefficient and gain obtained. It is observed that multiple bands are achieved from 2.6 GHz to 5.9 GHz with 15 bands, and the maximum gain is 11.0 dBi at 4.9 and 5.1 GHz, the results in current distribution enhancements that improve the antenna. All modeling has the exact dimensions.

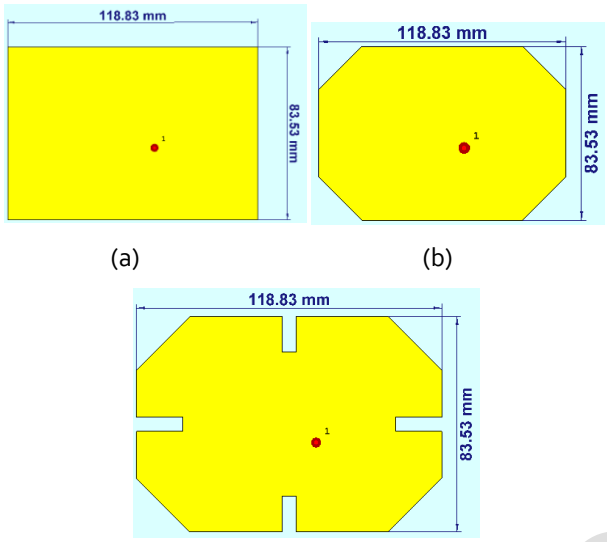

(a) (b)

(c)

Figure 3: The modeling of patch antenna a) the rectangle patch b) the cutting edge of rectangle c) the antenna proposal.

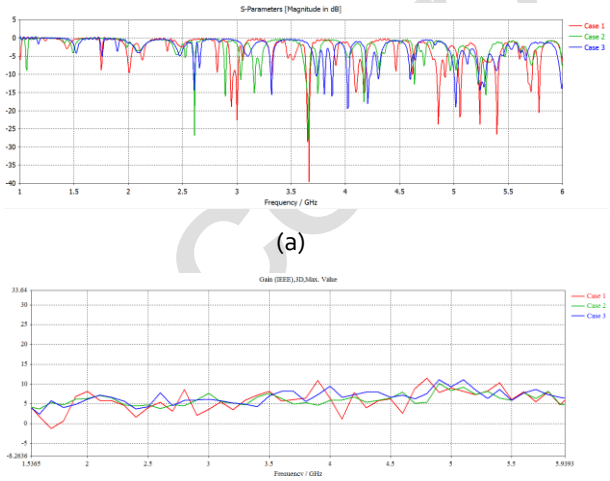

(a)

(b)

Figure 4: The parametric study of patch antenna (First Layer) a) reflection coefficient of antenna b) the gain of patch antenna.

3.2 The CRLH (second layer)

This section introduces the effects of the second layer of the proposed antenna on the antenna performance by increasing the number of facts (see Figure 5 (a and b). The reflection coefficient and gain spectra are calculated and presented in Figure 6(a and b). Based on the recorded results of mode 1, the reflection coefficient is reduced, and it sometimes shows a gain enhancement, as shown in Figure 5 (a). Next, in mode 2, further improvement in the reflection coefficient and gains are significantly observed. On the other hand, the radiation pattern in mode 2 does not originate at 1.9 GHz, whereas in mode 1, the radiation pattern is exhibited. On the other hand, the reflection coefficient of mode 1 has 12 multiband frequencies from 2.7 GHz to 5.5 GHz and 9 multiband frequencies in mode 2 from 2.6 GHz to 5.6 GHz. Furthermore, gain results in mode 2 are more improved than mode 3, where at the frequency of 3.1 GHz, the gain value attained to 6.37 dBi, and 3.1 GHz in mode 2, the gain is 8.14 dBi.

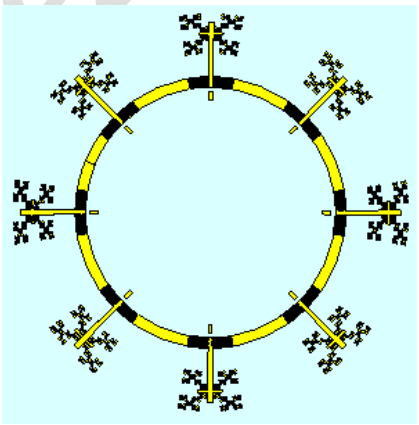

(a)

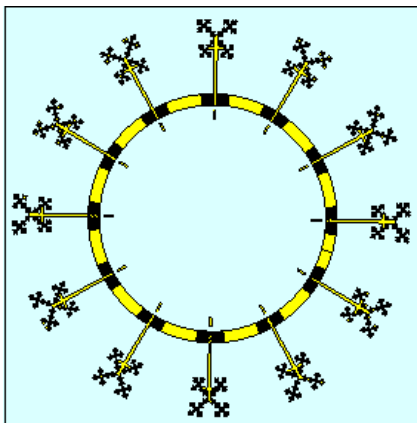

(b)

Figure 5: The CRLH structure (second layer) a) the 8 Fractal b) 12 Fractal.

Accepted article

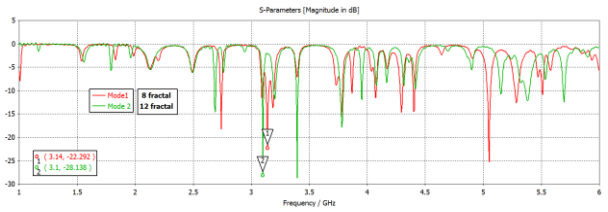

(a)

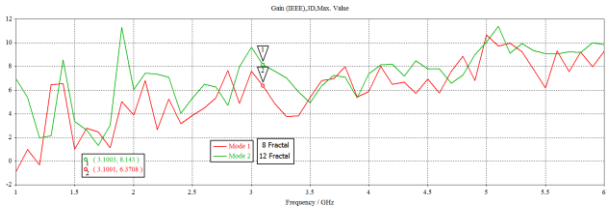

(b)

Figure 6: The CRLH structure (second layer) a) reflection coefficient results in b) gain result.

3.3 The MTS structures

This section considers the effect of the proposed MTS on the antenna performance with variation in the distance between the antenna from MTS and the second layer near and far between them (see Figure 7), which is also listed in Table 2. Mode 1 shows a minimized reflection coefficient than the rest modes and provides efficient gain at 4.4 GHz as well. Also, the gain in mode 2 is equal to 14.8 dB, where the MTS near the second layer is found as 25.33 mm with a similar value of the reflection coefficient in the case of mode 1. In addition, the gain decreases at mode 2 as compared with other modes, where the maximum gain at 3 GHz is 11.8 dBi. In mode 3, the MTS are far from the second layer with 60.25 mm. The reflection coefficient also still has the same value as mode 1. In the meantime, the gain value that is produced at this mode shows less than that at mode 1 and better than the gain at mode 2. The overall results are demonstrated in Figure 8.

Table 2 The distance between MTS and the second layer in all cases

Case	Value (mm)
Mode 1	40.28
Mode 2	25.23
Mode 3	60.25

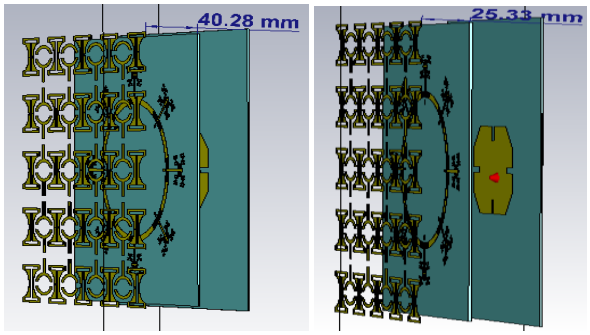

(a) (b)

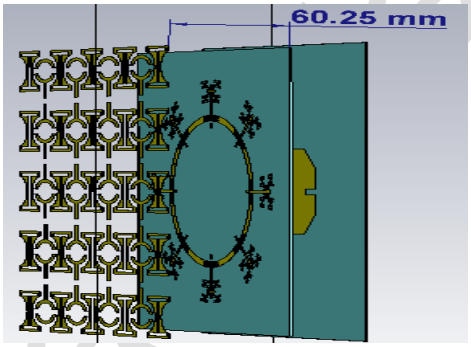

(c)

Figure 7: Distances of the MTS structure a) case 1 b) case 2 c) case 3

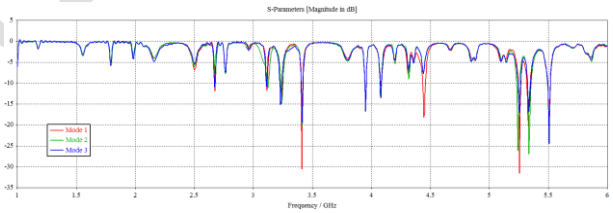

(a)

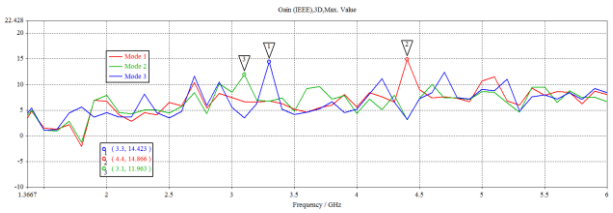

(b)

Figure 8: The result of MTS a) the Reflection coefficient of antenna b) the gain

Moreover, the radiation pattern at 4.4, 3.1, and 3.3 GHz are clearly illustrated in Figure 9.

Accepted article

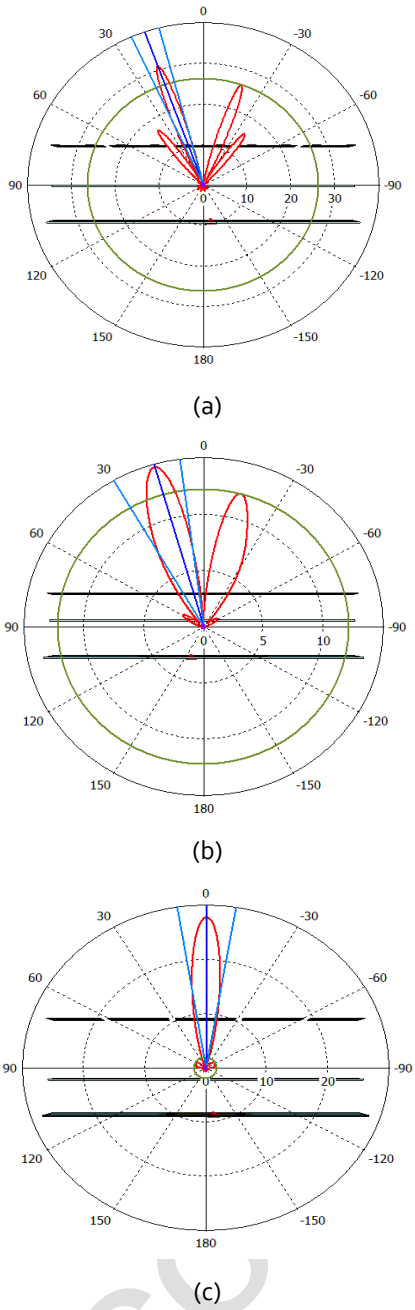

Figure 9: The radiation pattern of antenna at a) 4.4 GHz b) 3.1GHz c) 3.3 GHz

The methodology of the antenna design and the obtaining results are depicted in Figure 10.

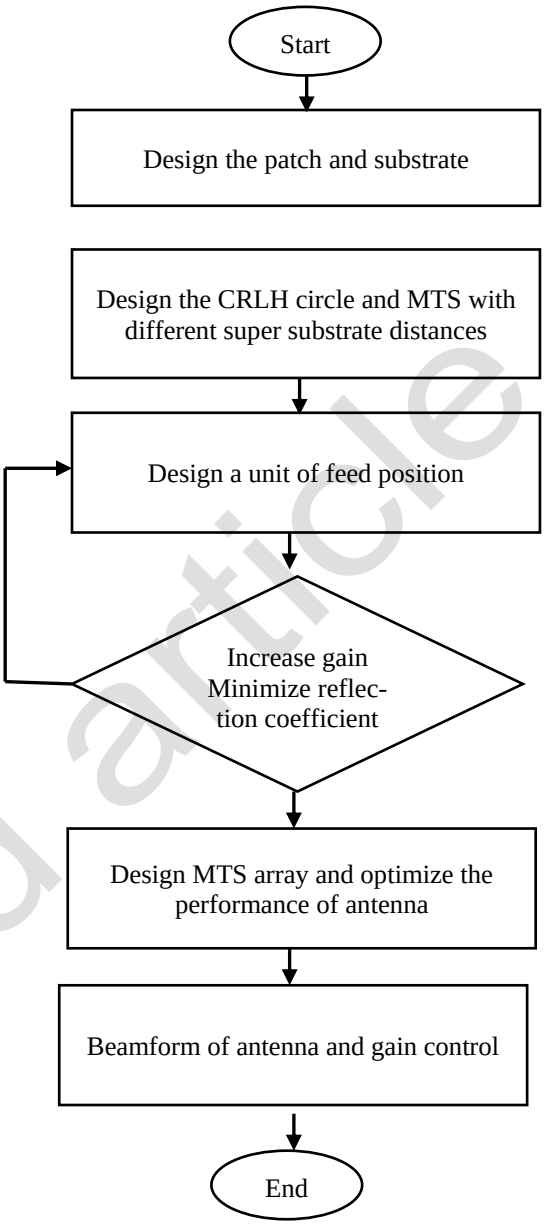

Figure 10: Flowchart of the antenna design

The proposed antenna performance based on the first layer is compared to the one based on the second layer of the fractal geometry and MTS layer, as seen in Figure. 11. The antenna performance in terms of the reflection coefficient spectrum is shown for each layer. A significant variation in the reflection coefficient spectra is found due to the individual introduction of each layer. The proposed antenna offers several frequency resonance modes with excellent matching of reflection coefficient magnitude below -10dB. Such achievements are attributed to the introduction of fractal geometry. The proposed structure is designed and analyzed using CST microwave studio. To excite the radiating structure, a 50Ω discrete port is assigned. The performance parameters, i.e., return loss, gain, and surface current

Accepted article

plots, are obtained using the standard boundary conditions in the CST microwave studio and powered by the circular patch. Therefore, a series of simulations were performed, as shown in Table 3—the PIN diode resistance and capacitance in the ON and OFF conditions. By controlling the biasing of the PIN diodes, the distribution of the antenna surface current will be modified; this will deflect the direction of the antenna radiation.

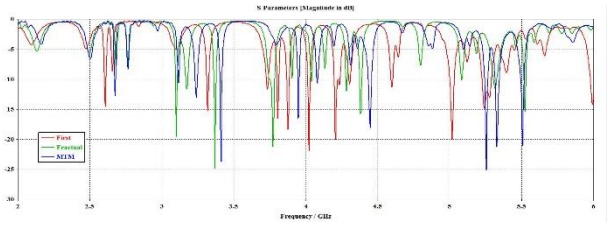

Figure 11: Reflection coefficient results

In the simulation environment, a parallel lumped RLC model with R, L, and C values shown in Figure 12 (a & b) mimics diodes ON and OFF states. It can be seen from Figure 12 (a) that in the ON state, an equivalent circuit having a series combination of 3Ω resistor and 2.6e-10 H inductor is modeled using parallel RLC boundary conditions. On the other hand, in the OFF state, a series combination of 0 H with a similar combination of 20 kΩ resistor and 0.04 pF capacitor, as depicted in Figure 12 (b), is modeled using RLC boundary conditions. The ON and OFF states of PIN diodes change the electrical length of the radiator to allow the appropriate low current density. Consequently, the ON and OFF states of pin diodes matched the impedance at different frequency bands at a time. They resulted in frequency reconfigurability at multiband depending upon the RF current.

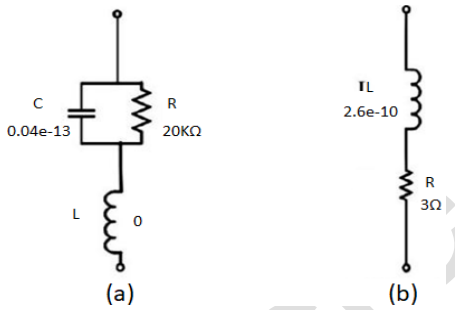

Figure 12: The RLC model operation of antenna: (a) OFF and (b) ON

The proposed antenna achieved reconfigurability by changing the diodes' switching process to offer an open and short circuit behavior between radiating patches. The antenna has five operating modes, each with a unique resonant frequency scheme. The conditions of the PIN diodes at each mode and respective deep bands are detailed in Table 3. Compared to other types of diodes, Varactor diodes are preferred to use in this work for the capability of producing voltage-controlled variable capacitance in radio frequency or RF circuits. These diodes also produce very little noise and are offered at a reduced cost.

Table 3: The statues of the antenna reconfiguration.

Case no.	Status of Pin diodes				Frequency/ GHz	Gain/ dBi
	P1	P2	P3	P4		
1	OFF	OFF	ON	ON	1.7,2.6,4	1.82,6.51,5.82
2	OFF	ON	OFF	ON	2.7,2.8,3.3	2.23,2.8,5.99
3	ON	ON	OFF	OFF	2.7,3.1,4.1	2.18,4.69,7.45
4	ON	OFF	ON	OFF	3.1	4.9
5	OFF	OFF	OFF	OFF	3.1,3.3,4.1,5.1,5.4	5.05,6.08,7.67,9.87,9.62
6	OFF	OFF	ON	OFF	4	7.68
7	ON	ON	ON	ON	2.7,2.8,3.1,4.1	2.48,2.81,
8	OFF	OFF	OFF	ON	1.8,2.7,3.1,3.3,4.1,5.1,5.4	0.19,2.23,5.27,5.95,7.2,11.1,8.81
9	ON	ON	ON	OFF	2.8,3.1	2.81,5.32
10	ON	OFF	ON	ON	1.8,2.7,3.1	0,1.24,4.97

The presented results in Table 2 illustrate that the proposed antenna has different operating modes. In Figure 13, the three studied cases show a maximum outcome variation. The obtained reflection coefficient indicates that the proposed antenna offers a wideband reconfigurability. For this, the antenna's best performance is achieved when all diodes are switched OFF.

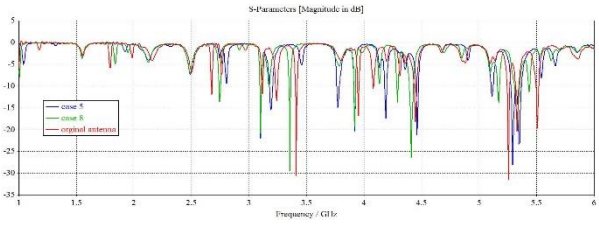

Accepted

Figure 13: Results of reflection coefficient for the three cases.

On the other hand, the antenna far-field radiation patterns are evaluated using an electromagnetic simulator from case 8. Figure 14 demonstrates the simulated radiation patterns generated by using the CST software. The main antenna beam is observed to be steered according to the switching conditions.

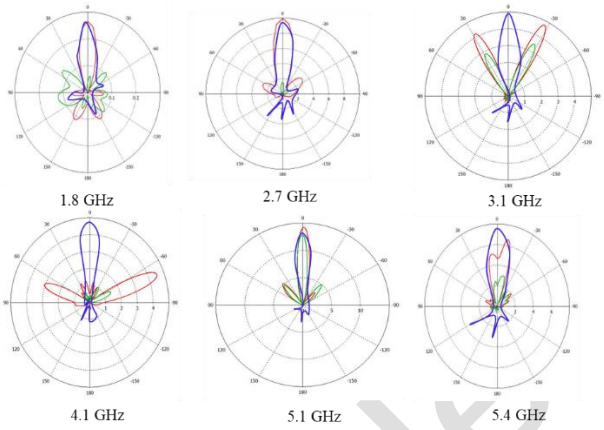

Figure 14. The antenna radiation pattern at different frequency bands.

To compare the proposed performance with other studies and with previously published research in the literature, Table 4 shows that the proposed antenna has a pattern-reconfigurability and enhanced gain and realizes a significant size reduction with less design complexity.

Table 4: Comparison between recently proposed antennas and the proposed.

Ref.	Frequency/ GHz	Reconfiguration	Technique	Gain/ dBi	PIN
[7]	3.1, 4.1, 3.8, 2.45, 7.8, 9.5	Frequency/ pattern	Hexagon/CPW	1.56, 4.24, 1.67, 1.68, 3.49, 1.69	2
[24]	2.4, 5.8	Frequency	slots	4	2
[1]	2.4, 5.8	Pattern	EBG	6.2, 6.6	14
[2]	2.6, 3.5, 4.2, 4.5, 5, 5.5	Frequency/ pattern	Parasitic/patch	1.72, 1.94, 2.51, 2.81, 3.66, 3.8	8
[4]	4.66, 5.2, 5.3, 5.8	Frequency	V-Shaped	3.4, 6	2
[5]	5.77-7.10	Frequency	Quasi-Yagi	5.7	4
[6]	5.8	Frequency/ pattern	Patch	5.95	4
[20]	2.6/4.2/5.6	Frequency	MS / super-substeate	8.2/4.49/6.24	3
[3]	2.3	Gain	Metamaterial	**6.15**	3
This work	1.8, 2.7, 3.1, 3.3, 4.1, 5.1, 5.4	Frequency/ pattern	diodes	0.19, 2.23, 5.27, 5.95, 7.2, 11.1, 8.81	4

4 Conclusion

This work proposes a reconfigurable antenna controlled using four PIN diodes for modern applications, including direct frequency multiplexing applications. This antenna is designed to operate for different frequency bands with acceptable gain. The antenna performance is very effective in the PIN diode switching change. The characteristics of each case are studied and discussed based on the simulation results obtained. The proposed antenna can be operated with the following frequencies: 1.8 GHz, 2.7 GHz, 3.1 GHz, 3.3 GHz, 4.1 GHz, 5.1 GHz, and 5.4 GHz. Additionally, the antenna achieved an agreement gain of up to 11.1 dBi at 5.1 GHz and 8.81 dBi at 5.2 GHz. Compared with other related published papers, this antenna exhibits less complexity and is highly efficient for different applications.

Accepted article

5 Conflict of Interest

The authors declare no conflict of interest.

6 References

[1] J. Zhu, C.-H. Chu, L. Deng, C. Zhang, Y. Yang, and S. Li, "mm-Wave high gain cavity-backed aperture-coupled patch antenna array," *IEEE Access,* vol. 6, pp. 44050-44058, 2018.

[2] J. Khan, S. Ullah, U. Ali, F. A. Tahir, I. Peter, and L. Matekovits, "Design of a millimeter-wave MIMO antenna array for 5G communication terminals," *Sensors,* vol. 22, no. 7, p. 2768, 2022.

[3] B. S. Bashar, Z. Rhazali, H. Misran, M. M. Ismail, and M. T. Al-Sharify, "Gain enhancement for patch antenna loading with slotted parasite antenna based on metasurface super substrate," in *AIP Conference Proceedings*, 2023, vol. 2787, no. 1: AIP Publishing.

[4] K. Raheel *et al.*, "E-shaped H-slotted dual band mmWave antenna for 5G technology," *Electronics,* vol. 10, no. 9, p. 1019, 2021.

[5] H. Ullah and F. A. Tahir, "A broadband wire hexagon antenna array for future 5G communications in 28 GHz band," *Microwave and Optical Technology Letters,* vol. 61, no. 3, pp. 696-701, 2019.

[6] Q. Zhu, K. B. Ng, C. H. Chan, and K.-M. Luk, "Substrate-integrated-waveguide-fed array antenna covering 57–71 GHz band for 5G applications," *IEEE Transactions on Antennas and Propagation,* vol. 65, no. 12, pp. 6298-6306, 2017.

[7] C.-X. Mao, S. Gao, and Y. Wang, "Broadband high-gain beam-scanning antenna array for millimeter-wave applications," *IEEE Transactions on Antennas and Propagation,* vol. 65, no. 9, pp. 4864-4868, 2017.

[8] B. Batagelj, "Centimeter positioning accuracy in modern wireless cellular networks–wish or reality?," *Informacije MIDEM,* vol. 53, no. 4, pp. 239-248, 2023.

[9] H. Ullah and F. A. Tahir, "A novel snowflake fractal antenna for dual-beam applications in 28 GHz band," *IEEE Access,* vol. 8, pp. 19873-19879, 2020.

[10] E. G. Larsson, O. Edfors, F. Tufvesson, and T. L. Marzetta, "Massive MIMO for next generation wireless systems," *IEEE communications magazine,* vol. 52, no. 2, pp. 186-195, 2014.

[11] S. Shamim, U. S. Dina, N. Arafin, and S. Sultana, "Design of efficient 37 GHz millimeter wave microstrip patch antenna for 5G mobile application," *Plasmonics,* vol. 16, no. 4, pp. 1417-1425, 2021.

[12] R. Rashmitha, N. Niran, A. A. Jugale, and M. R. Ahmed, "Microstrip patch antenna design for fixed mobile and satellite 5G communications," *Procedia Computer Science,* vol. 171, pp. 2073-2079, 2020.

[13] N. Ojaroudiparchin, M. Shen, and G. F. Pedersen, "Beam-steerable microstrip-fed bow-tie antenna array for fifth generation cellular communications," in *2016 10th European Conference on Antennas and Propagation (EuCAP)*, 2016: IEEE, pp. 1-5.

[14] M. El Shorbagy, R. M. Shubair, M. I. AlHajri, and N. K. Mallat, "On the design of millimetre-wave antennas for 5G," in *2016 16th Mediterranean Microwave Symposium (MMS)*, 2016: IEEE, pp. 1-4.

[15] I. Elfergani, A. S. Hussaini, A. M. Abdalla, J. Rodriguez, and R. Abd-Alhameed, "Millimeter wave antenna design for 5G applications," *Optical and Wireless Convergence for 5G Networks,* pp. 139-156, 2019.

[16] M. Ur-Rehman, Q. H. Abbasi, A. Rahman, I. Khan, H. T. Chattha, and M. A. Matin, "Millimetre-wave antennas and systems for the future 5G," vol. 2017, ed: Hindawi, 2017.

[17] A. R. Al-tameemi *et al.*, "A Novel Conformal MIMO Antenna Array based a Cylindrical Configuration for 5G Applications," in *2022 9th International Conference on Electrical Engineering, Computer Science and Informatics (EECSI)*, 2022: IEEE, pp. 446-451.

[18] J. Zhang, X. Ge, Q. Li, M. Guizani, and Y. Zhang, "5G millimeter-wave antenna array: Design and challenges," *IEEE Wireless communications,* vol. 24, no. 2, pp. 106-112, 2016.

[19] K. Bangash, M. M. Ali, H. Maab, and R. A. Shaukat, "Effect of embedding H-Shaped slot on the characteristics of millimeter wave microstrip patch antenna for 5G applications," in *2019 2nd International Conference on Computing, Mathematics and Engineering Technologies (iCoMET)*, 2019: IEEE, pp. 1-4.

[20] B. S. Bashar *et al.*, "Antenna beam forming technology based enhanced metamaterial superstrates," in *2022 IEEE 3rd KhPI Week on Advanced Technology (KhPIWeek)*, 2022: IEEE, pp. 1-5.

[21] K. Bangash, M. M. Ali, H. Maab, and H. Ahmed, "Design of a millimeter wave microstrip patch antenna and its array for 5g applications," in *2019 International Conference on Electrical, Communication, and Computer Engineering (ICECCE)*, 2019: IEEE, pp. 1-6.

Accepted article

[22] R. Przesmycki, M. Bugaj, and L. Nowosielski, "Broadband microstrip antenna for 5G wireless systems operating at 28 GHz," *Electronics,* vol. 10, no. 1, p. 1, 2020.

[23] M. Atanasijević-Kunc, V. Kunc, and M. Štiglic, "AUTOMATIC TUNING OF ELECTRICAL SMALL ANTENNAS," *Informacije MIDEM,* vol. 40, no. 3, pp. 174-177, 2010.

[24] Z. Lodro, N. Shah, E. Mahar, S. B. Tirmizi, and M. Lodro, "mmWave novel multiband microstrip patch antenna design for 5G communication," in *2019 2nd International conference on computing, mathematics and engineering technologies (iCoMET)*, 2019: IEEE, pp. 1-4.

[25] Z. Wang, J. Liu, J. Wang, and G. Yue, "Beam squint effect on high-throughput millimeter-wave communication with an ultra-massive phased array," *Frontiers of Information Technology & Electronic Engineering,* vol. 22, no. 4, pp. 560-570, 2021.

[26] I. Laurinavicius, H. Zhu, J. Wang, and Y. Pan, "Beam squint exploitation for linear phased arrays in a mmWave multi-carrier system," in *2019 IEEE Global Communications Conference (GLOBECOM)*, 2019: IEEE, pp. 1-6.

[27] S. Glinsek, V. Furlan, T. Pecnik, M. Vidmar, B. Kmet, and B. Malic, "Elliptically polarized frequency agile antenna on ferroelectric substrate," *Informacije MIDEM,* vol. 48, no. 4, pp. 229-233, 2018.

[28] S. Rangan, T. S. Rappaport, and E. Erkip, "Millimeter-wave cellular wireless networks: Potentials and challenges," *Proceedings of the IEEE,* vol. 102, no. 3, pp. 366-385, 2014.

Copyright © 20xx by the Authors. This is an open access article distributed under the Creative Commons Attribution (CC BY) License (https://creativecommons.org/licenses/by/4.0/), which permits unrestricted use, distribution, and reproduction in any medium, provided the original work is properly cited.

Arrived: 17.01.2024
Accepted: 22.03.2024

Accepted article